

# Quantum entanglement distribution with 810 nm photons through telecom fibers

E. Meyer-Scott,<sup>1</sup> H. Hübel,<sup>1</sup> A. Fedrizzi,<sup>2</sup> C. Erven,<sup>1</sup> G. Weihs,<sup>3,1</sup> and T. Jennewein<sup>1</sup>

<sup>1</sup>*Institute for Quantum Computing, University of Waterloo,  
200 University Avenue W, Waterloo N2L 3G1, Canada\**

<sup>2</sup>*Department of Physics and Centre for Quantum Computer Technology,  
University of Queensland, Brisbane QLD 4072, Australia*

<sup>3</sup>*Institute für Experimentalphysik, Universität Innsbruck, Technikerstrasse 25, 6020 Innsbruck, Austria*

We demonstrate the distribution of polarization entangled photons of wavelength 810 nm through standard telecom fibers. This technique allows quantum communication protocols to be performed over established fiber infrastructure, and makes use of the smaller and better performing setups available around 800 nm, as compared to those which use telecom wavelengths around 1550 nm. We examine the excitation and subsequent quenching of higher-order spatial modes in telecom fibers up to 6 km in length, and perform a distribution of high quality entanglement (visibility 95.6%). Finally, we demonstrate quantum key distribution using entangled 810 nm photons over a 4.4 km long installed telecom fiber link.

The ability to distribute entanglement is an important building block in the field of quantum information processing. It is employed in protocols such as quantum teleportation[1], quantum key distribution (QKD)[2], and quantum computing [3]. Many quantum information experiments so far have been performed at wavelengths around 800 nm, making use of the high performance (low noise, high speed, and around 70% efficiency) of silicon avalanche photodiodes (Si-APDs) for single-photon detection. Such systems have been demonstrated in laboratories, over free space links [4, 5] or with custom laid 800 nm single mode fibers[6], the latter of which face the difficulty of installing a dedicated link. In addition, most quantum memory implementations and quantum dot photon-sources are designed around 800 nm optical transitions[7]. On the other hand, quantum communication setups have been built to make use of existing telecom fiber infrastructure and low fiber loss at 1550 nm[8]; however, single-photon detectors based on APDs designed for these wavelengths (InGaAs-APDs) add considerable complexity, require elaborate synchronization of detector gates, and suffer from low detector efficiencies ( $\sim 15\%$ ). In fact, based on the efficiencies above, and fiber losses of 3 dB/km for 800 nm light and 0.22 dB/km for 1550 nm light, overall attenuation will be lower for 800 nm photons for up to 7.3 dB of fiber losses, corresponding to 2.4 km of telecom fiber. In spite of the common perception that entanglement distribution at 800 nm strictly requires wavelength-specific components, it is obvious that such short wavelength systems would greatly benefit if used with the existing fiber infrastructure. Toward this goal we report on the high fidelity distribution of entangled photon pairs at 810 nm through several kilometers of standard telecom fibers, which provides a path for demonstrating quantum information applications, like entanglement based QKD, and other quantum optics experiments in existing fiber networks.

We adapted a polarization-entanglement based quantum communication system[9] at 810 nm using the BBM92 protocol[10] to transmit photons to Alice and Bob through varying lengths of single mode telecom fibers [mode field diameter (MFD) of  $9.2 \mu\text{m}$ ] ranging from 250 m to 6000 m (Fig. 1) or short stretches of 810 nm single mode fibers with a MFD of  $5.4 \mu\text{m}$ . After transmission through the fibers, each photon of the entangled pair passes through a polarization analyzing module, which forwards the photons to one of four Si-APDs, depending on the measured polarization state ( $0^\circ$ ,  $90^\circ$ ,  $45^\circ$  or  $-45^\circ$ ). A time-tagging unit then records the state and the time of the detection. This information is bundled and passed to Alice and Bob's computers, which communicate classically to find the optimal time offset to maximize the number of coincidences between Alice's and Bob's detection events.

Since standard telecom fiber is slightly multimode for 810 nm light we expect the appearance of higher-order spatial modes. Guided wave theory predicts two linearly polarized modes of propagation ( $LP_{01}$  and  $LP_{11}$ ) [11] for

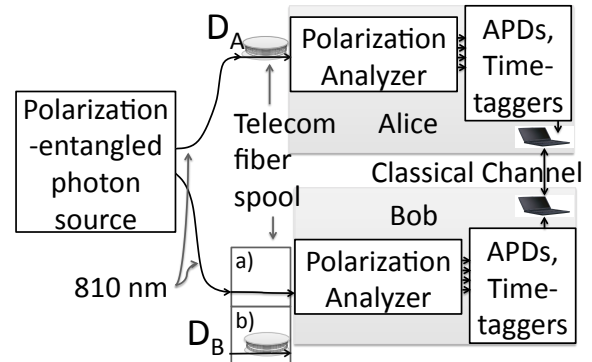


FIG. 1: Schematic of setup. (a) Asymmetric distribution scheme, with only a short 810 nm single mode fiber to Bob. (b) Symmetric scheme, with long 1550 nm telecom fibers to both Alice (length  $D_A$ ) and Bob (length  $D_B$ )

\*Electronic address: emeyersc@iqc.ca

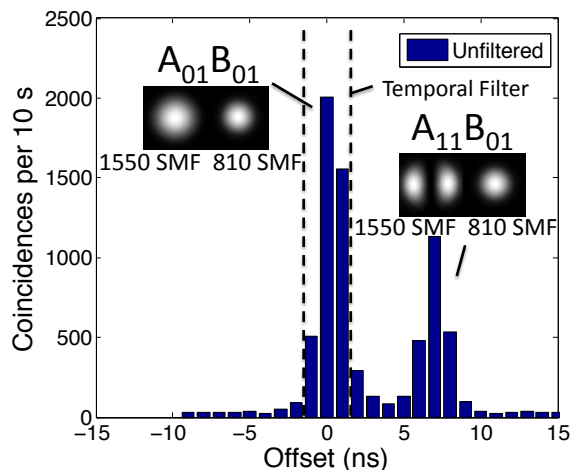


FIG. 2: Asymmetric distribution ( $D_A=3$  km,  $D_B=0$  km): histogram of coincident detection events with delay between Alice's and Bob's detection. The slower  $A_{11}$  mode in Alice's arm is intentionally excited to illustrate the effect, then filtered. The theoretical power distribution of the propagating spatial modes at 810 nm for different fibers types is inset.

810 nm photons in a telecom fiber. Here the modes are labeled based on the distribution arm (Alice or Bob) and the azimuthal index  $i$  (e.g.,  $A_{i1}$ ). The two propagation modes show modal dispersion; i.e., the group velocity of the  $A_{11}$  mode is different from that of the  $A_{01}$  mode, resulting in two distinct arrival times [12]. Detecting Bob's photons locally and Alice's after 3 km of telecom fiber resulted in a histogram of coincidences with two pronounced peaks, as seen in Fig. 2. The relative offset of the two peaks varied linearly with fiber length leading to a measured modal dispersion of 2.20 ns/km, in excellent agreement with the theoretical value of 2.19 ns/km. As evidenced by the well-defined peaks in Fig. 2, there is little crosstalk between the two modes after the initial insertion, so the polarization state in the fundamental mode is well preserved and the timing signature of each mode is evident.

For a high fidelity transmission of polarization entangled photons it is necessary to select only the fundamental mode in both arms ( $A_{01}B_{01}$ ), as higher order modes will lead to an increased error in the polarization contrast since only one of the polarization rotations experienced by different modes in the fiber can be compensated for. In principle, the modes could be separated and compensated individually, but without such elaborate mode extraction two methods for filtering out the higher modes at the receiver are developed:

(i) In the case of an asymmetric distribution, where the fiber lengths to Alice and Bob are not identical, a temporal filter can be applied in the form of a narrow coincidence window, which will cut out the higher order peak, as demonstrated in Fig. 2. This technique introduces no additional optical losses.

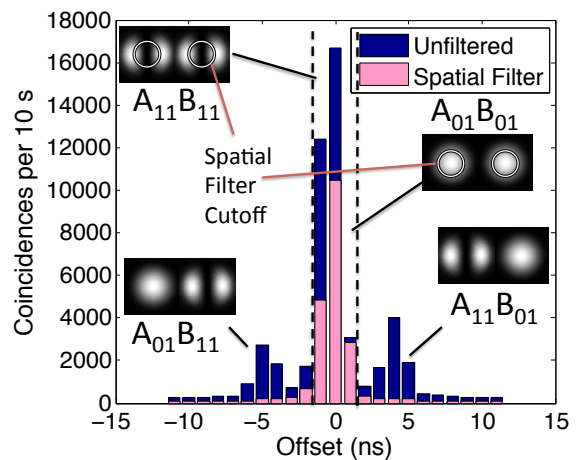


FIG. 3: Symmetric distribution ( $D_A=2$  km,  $D_B=2$  km): selection of  $A_{01}B_{01}$  mode by spatial filtering. The spatial filter (core radius superimposed on power distribution) eliminates not only the side peaks (due to photons coupling into cross modes) but also those coincidences in the central peak that are a result of both photons coupling into the higher mode ( $A_{11}B_{11}$ ), such that they give little or no betraying time offset.

(ii) In a symmetric distribution, where both Alice and Bob receive photons through telecom fiber and where the difference in fiber lengths is less than 2 km, the  $A_{01}B_{01}$  and  $A_{11}B_{11}$  peaks become inseparable in time, as seen in the central peak of Fig. 3. In this case, in addition to the temporal filter to eliminate the side peaks, a spatial filter (810 nm single mode fiber) is used before detection. Since the radial extent of the power in the higher order modes is greater than that in the fundamental mode, the smaller core of the 810 nm fiber (shown as a ring in Fig. 3) removes around 98% of the  $A_{11}$  or  $B_{11}$  mode while preserving at least 75% of the  $A_{01}$  or  $B_{01}$  mode.

In order to quantify our filtering methods we performed entanglement distribution measurements with telecom fiber spools of lengths up to  $D_A=6$  km (asymmetrically), and up to  $D_A=D_B=2$  km (symmetrically). We extracted the entanglement visibility (a measure of the quality of entanglement)[8], raw coincidences, and secure key rate for QKD based on realistic error correction and privacy amplification[13] (Table I). To set a benchmark for comparison, measurements were performed locally with short 810 nm fibers (2 m), resulting in  $95.7\pm 0.4\%$  visibility<sup>1</sup>.

For the asymmetric distribution we employed a 3 ns coincidence window as the temporal filter: at 2 km of fiber in one arm, for example, overall visibility was improved from 88.0% to 94.6% with this method. Figure 4 shows

<sup>1</sup> Differences in count rates are due to a realignment of the source between measurements.

TABLE I: Summary of entanglement distribution for various telecom fiber lengths, including QKD key rates. Transmission loss includes attenuation in the optical fibers, as well as loss from the filtering processes. Local measurements gave an average visibility of  $95.7\pm 0.4\%$ . Uncertainty is taken as due to Poissonian count fluctuations.

Distribution Scheme	$D_A$ (km)	$D_B$ (km)	Transmission Loss (dB)	Filtering	Visibility (%)	Coinc. (rate/s)	Secure Key (rate/s)
Asymmetric	2.0	0.0	6	None	$88.0\pm 0.2$	3000	420
			7	Temporal	$94.6\pm 0.2$	2700	800
Asymmetric	5.0	0.0	15	Temporal	$91.6\pm 0.5$	430	90
Symmetric	2.0	2.0	12	None	$62.9\pm 0.4$	5200	0
			14	Temporal	$92.2\pm 0.3$	3600	850
			16	Temporal+spatial	$95.6\pm 0.2$	1950	650

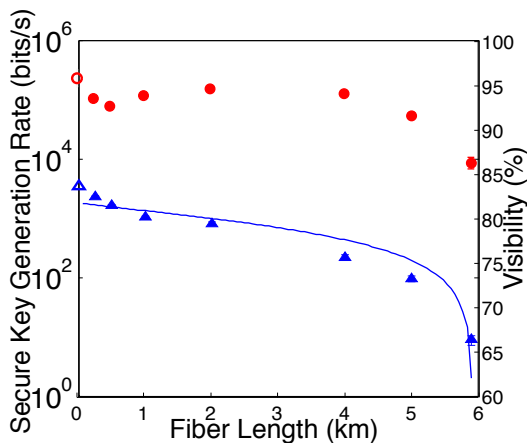


FIG. 4: Secure key generation rates (triangles) and measured visibility (circles) as a function of fiber length in Alice’s arm. The open symbols are local data, and the line is a fit to the secure key rate with realistic parameters (see Ref. 13). Error bars are smaller than symbol size.

the visibility for asymmetric distribution distances up to 6 km. Figure 4 also shows a calculated QKD secure key rate, dropping linearly (on the log scale) with increasing lengths of fibers, with a sharp cut-off around 6 km due to increased loss and detector dark counts.

In the case of symmetric distribution (see Table I), we employed both filtering techniques to raise visibility from 62% to 95.6%. For this and the asymmetric case, visibility is brought close to the benchmark which implies that the higher order modes are suppressed using the filtering detailed above, and that there is no significant crosstalk along the length of the fiber.

To illustrate the utility of this form of entanglement distribution, we performed a full QKD protocol over two symmetric 2.2 km channels of installed telecom fibers. Two parallel fibers were used between the Mathematics and Computer Building on the University of Waterloo’s campus (source of entangled photons) and the Perimeter Institute (detection modules Alice and Bob), leading to a total distribution distance of 4.4 km. The quantum bit error ratio (QBER) was higher than for the fiber spools, likely due to disturbances from passing cars, trains, and thermal fluctuations. For example, over 15 min, the average QBER was 4.3% (i.e., 91.4% visibility) with both temporal and spatial filtering, leading to an average secure key rate of 350 bits/s (see Fig. 5). During longer runs, the errors tended to increase with time due to polarization drifts in the fibers.

Our approach has the potential for much higher dis-

tribution rates, as local coincidence rates of 2.5 MHz have been achieved with short-wavelength entanglement sources [14]. Assuming the same fiber loss observed here, secure key rates of 500 kb/s are possible over a 4 km symmetric link using only standard telecom fibers. Previous systems based on weak laser pulses around 800 nm were

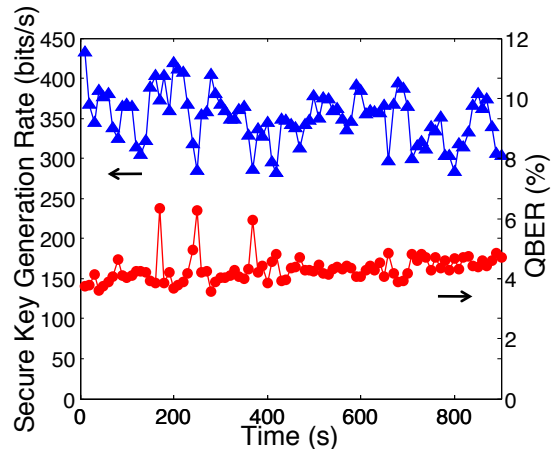


FIG. 5: Secure key generation rate and measured QBER in a symmetric installed fiber link. Each data point is the average over 20 s.

limited to key rates of 100 kb/s over 4 km of telecom fiber [15]. Given the superior functionality and lower complexity of detectors at 800 nm combined with the multiuser networking capabilities of entanglement [16], we believe that such QKD systems will find applications in inner city links or corporate networks. In addition, the possibility to address multiple modes in a fiber could be useful for implementations of higher-dimensional quantum information.

We have demonstrated the viability of entanglement distribution in standard optical fibers using 810 nm photons. With suitable filtering, error rates are not affected by higher order modes in the fiber and high fidelity distribution can be achieved over several kilometers. We believe our results pave the way for a wide usage of telecom optical infrastructure together with the well established quantum information systems at shorter wavelengths.

The authors would like to thank Allison MacDonald for calculations, Greg Cummings and Bruce Campbell of IST UW, John McCormick, Joy Montgomery, Hon Lau, and Joe Stauttner of IT at PI, Châteauneuf François of INO for test fibers, NSERC (CGS, PGS, QuantumWorks, Discovery), OCE, CIFAR, CFI, and ERA for funding.

[1] D. Bouwmeester, J.-W. Pan, K. Mattle, M. Eibl, H. Weinfurter, and A. Zeilinger, *Nature* **390**, 575 (1997), .  
 [2] N. Gisin, G. Ribordy, W. Tittel, and H. Zbinden, *Rev.*

*Mod. Phys.* **74**, 145 (2002).

[3] E. Knill, R. Laflamme, and G. J. Milburn, *Nature* **409**, 46 (2001), .

- [4] C. Kurtsiefer, P. Zarda, M. Halder, H. Weinfurter, P. M. Gorman, P. R. Tapster, and J. G. Rarity, *Nature* **419**, 450 (2002), .
- [5] R. Ursin, F. Tiefenbacher, T. Schmitt-Manderbach, H. Weier, T. Scheidl, M. Lindenthal, B. Blauensteiner, T. Jennewein, J. Perdigues, P. Trojek, et al., *NATURE PHYSICS* **3**, 481 (2007), .
- [6] A. Poppe, A. Fedrizzi, R. Ursin, H. Böhm, T. Lörünser, O. Maurhardt, M. Peev, M. Suda, C. Kurtsiefer, H. Weinfurter, et al., *Opt. Express* **12**, 3865 (2004), .
- [7] Z.-S. Yuan, Y.-A. Chen, B. Zhao, S. Chen, J. Schmiedmayer, and J.-W. Pan, *Nature* **454**, 1098 (2008), .
- [8] H. Hübel, M. R. Vanner, T. Lederer, B. Blauensteiner, T. Lörünser, A. Poppe, and A. Zeilinger, *Opt. Express* **15**, 7853 (2007), .
- [9] C. Erven, C. Couteau, R. Laflamme, and G. Weihs, *Opt. Express* **16**, 16840 (2008).
- [10] C. H. Bennett, G. Brassard, and N. D. Mermin, *Physical Review Letters* **68** (1992), .
- [11] B. E. A. Saleh and M. C. Teich, *Fundamentals of Photonics* (Wiley, 2007), 2nd ed.
- [12] P. D. Townsend, *Photonics Technology Letters*, IEEE **10**, 1048 (1998).
- [13] X. Ma, C.-H. F. Fung, and H.-K. Lo, *Physical Review A* **76**, 012307 (2007).
- [14] T. Scheidl, R. Ursin, A. Fedrizzi, S. Ramelow, X.-S. Ma, T. Herbst, R. Prevedel, L. Ratschbacher, J. Kofler, T. Jennewein, et al., *New Journal of Physics* **11**, 085002 (13pp) (2009), .
- [15] R. Collins, R. Hadfield, V. Fernandez, S. Nam, and G. Buller, *Electronics Letters* **43**, 180 (2007), .
- [16] H. C. Lim, A. Yoshizawa, H. Tsuchida, and K. Kikuchi, *Opt. Express* **16**, 14512 (2008), .